AAAS
Ultrafast Science
Volume 2022, Article ID 9761458, 8 pages
https://doi.org/10.34133/2022/9761458

Ultrafast Science
A SCIENCE PARTNER JOURNAL

Research Article

High-Sensitivity Gas Detection with Air-Lasing-Assisted Coherent Raman Spectroscopy

Zhihao Zhang,[1,2,3] Fangbo Zhang,[1,2] Bo Xu,[1,2] Hongqiang Xie,[1,4] Botao Fu,[1,2,3] Xu Lu,[1,2] Ning Zhang,[1,2] Shupeng Yu,[1,2] Jinping Yao,[1] Ya Cheng,[1] and Zhizhan Xu[1]

[1]*State Key Laboratory of High Field Laser Physics, Shanghai Institute of Optics and Fine Mechanics, Chinese Academy of Sciences, Shanghai 201800, China*
[2]*University of Chinese Academy of Sciences, Beijing 100049, China*
[3]*School of Physical Science and Technology, ShanghaiTech University, Shanghai 200031, China*
[4]*School of Science, East China University of Technology, Nanchang 330013, China*

Correspondence should be addressed to Jinping Yao; jinpingmrg@163.com, Ya Cheng; ya.cheng@siom.ac.cn, and Zhizhan Xu; zzxu@mail.shcnc.ac.cn

Zhihao Zhang and Fangbo Zhang contributed equally to this work.

Received 8 November 2021; Accepted 28 February 2022; Published 8 April 2022

Remote or standoff detection of greenhouse gases, air pollutants, and biological agents with innovative ultrafast laser technology attracts growing interests in recent years. Hybrid femtosecond/picosecond coherent Raman spectroscopy is considered as one of the most versatile techniques due to its great advantages in terms of detection sensitivity and chemical specificity. However, the simultaneous requirement for the femtosecond pump and the picosecond probe increases the complexity of optical system. Herein, we demonstrate that air lasing naturally created inside a filament can serve as an ideal light source to probe Raman coherence excited by the femtosecond pump, producing coherent Raman signal with molecular vibrational signatures. The combination of pulse self-compression effect and air lasing action during filamentation improves Raman excitation efficiency and greatly simplifies the experimental setup. The air-lasing-assisted Raman spectroscopy was applied to quantitatively detect greenhouse gases mixed in air, and it was found that the minimum detectable concentrations of CO_2 and SF_6 can reach 0.1% and 0.03%, respectively. The ingenious designs, especially the optimization of pump-seed delay and the choice of perpendicular polarization, ensure a high detection sensitivity and signal stability. Moreover, it is demonstrated that this method can be used for simultaneously measuring CO_2 and SF_6 gases and distinguishing $^{12}CO_2$ and $^{13}CO_2$. The developed scheme provides a new route for high-sensitivity standoff detection and combustion diagnosis.

1. Introduction

Remote detection and identification of atmospheric pollutants and hazardous biochemical agents are of fundamental importance for environmental science and national defense security. The innovative advances in ultrafast laser technologies over the past three decades provide new strategies to meet the urgent needs of various environmental and security issues. It is well known that high-energy femtosecond laser pulses could propagate over a long distance with a high intensity of 10^{13}~10^{14} W/cm^2, giving rise to filamentation phenomenon [1–3]. In the last few decades, femtosecond laser filamentation has shown the promising applications in many fields such as gas detection [4], weather control [5], remote fabrication [6], and laser ignition [7]. Particularly, filament-based gas sensing shows attractive prospects due to the long-distance propagation advantage of femtosecond laser filamentation as well as the ability to generate supercontinuum radiation and clean fluorescence signals [4, 5]. Commonly, filament-based remote sensing is realized by measuring characteristic fluorescence radiation [8–11] or intrinsic absorption [12] of the detected species. For example, Xu et al. detected CH_4 with the 2.6% concentration using the laser-induced fluorescence [9] and demonstrated

the feasibility of this method in multicomponent analysis [10]. The femtosecond laser filamentation is also accompanied by the supercontinuum coherent radiation, which offers a natural white-light source at a remote location. Kasparian et al. retrieved the distributions of atmospheric temperature and content of water vapor by recording the backscattered white-light absorption spectrum from 4.5 km altitude [12].

Besides the fluorescence and absorption spectroscopy, coherent anti-Stokes Raman scattering (CARS) is also a benchmark approach widely applied in gas sensing [13, 14]. Among the various CARS configurations, the hybrid femtosecond/picosecond (fs/ps) CARS is considered as one of the most sophisticated spectroscopic techniques [15–18]. The technique shares the advantages of impulsive Raman excitation with a femtosecond laser and high spectral resolution with a picosecond laser and allows for the background suppression by the flexible control of pump-probe delay. It thus has a high signal-to-noise ratio (SNR), a good chemical specificity, and abilities of temporal and spectral resolutions. In the hybrid fs/ps CARS scheme, the picosecond probe pulses are usually acquired by either spectrally narrowing a femtosecond laser [15–17] or adopting an additional picosecond laser [18]. The complicated experimental device hinders its broad applications under complex or dangerous environments.

The discovery and extensive investigation of air lasing [19–30] in recent years open an exciting perspective for atmospheric remote sensing due to its ability of generating cavity-free light amplification in the open air. Particularly, some unique properties (e.g., the narrow spectrum, natural spatial overlap with the femtosecond driver laser, intrinsic delay with respect to the driver laser, and asymmetric temporal envelope) [20, 21, 31–33] make it suitable as a probe to interrogate the Raman coherence. Hence, since air lasing was experimentally demonstrated, significant efforts have been paid to its applications in Raman spectroscopy [34–39]. With the nitrogen laser produced in N_2-Ar gas mixture, Malevich et al. performed a proof-of-principle experiment of gas sensing by measuring Raman gain or loss [35]. The N_2^+ lasing was also used for probing rotational coherence of N_2 and CO_2 molecules [34, 37]. Liu et al. observed the cascaded rotational Raman scattering as high as 58 orders by using air lasing as a probe [37]. Recently, Zhao et al. successfully detected vibrational Raman signals of CO_2 and CH_4 mixed in air with the assistance of N_2^+ lasing [39]. These studies show the feasibility of air-lasing-assisted Raman spectroscopy used for gaseous detection. However, all these studies were carried out in either pure or high-concentration gas molecules. The poor SNR and large signal fluctuations inevitably brought by the femtosecond laser filamentation cannot meet the requirements of practical applications. Therefore, it still remains challenging to improve the sensitivity and stability of filament-based ultrafast spectroscopy while exploiting its remarkable advantages.

In this Letter, we developed a high-sensitivity air-lasing-assisted CARS technique and further applied it to carry out quantitative analysis of greenhouse gas concentration. In the developed technique, the external-seed amplification mechanism was adopted to improve the strength of N_2^+ lasing as well as SNR of Raman scattering, and the orthogonal polarization arrangement was exploited to suppress the supercontinuum background. These specific designs greatly improve the sensitivity and stability of gas detection. It turns out that this technique can be used to detect the greenhouse gas with a concentration as low as 0.03% mixed in air. Besides, multicomponent detection and isotope identification were realized via the developed method. Therefore, this work takes an important step for the application of the advanced ultrafast laser spectroscopy in standoff detection of atmospheric trace gases, air pollutants, and toxic substances.

2. Basic Principle and Methods

2.1. Experimental Design. The experiment was performed by using a commercial Ti:sapphire laser system (Libra, Coherent, Inc.), which delivers 800 nm, 50 fs laser pulses with a maximum pulse energy of ~4 mJ at a repetition rate of 1 kHz. As shown in Figure 1, the output laser was split into two beams. One beam with the energy of 3.65 mJ served as the pump, which establishes the vibrational coherence of the target molecules as well as induces optical gain for the follow-up seed amplification in N_2^+. Another beam was focused by a lens with $f = 20$ cm and then was collimated by a lens with $f = 10$ cm. A sapphire plate was placed near the focus of the first lens to broaden the spectrum of the 800 nm femtosecond laser. The spectrally broadened laser was launched into a 1 mm thick BBO crystal to produce a seed pulse at 428 nm. The seed pulse was significantly amplified in air, giving rise to N_2^+ lasing, which serves as the probe of coherent Raman scattering. The pump-seed delay was controlled with a motorized translation stage. The two beams were collinearly focused into the gas chamber filled with a mixture of the target gas and standard air containing ~80% nitrogen and ~20% oxygen by using a lens with an optimal focal length of 14 cm. The pressure of the gas mixture was kept at atmospheric pressure for all measurements. Greenhouse gases CO_2 and SF_6 were chosen as target molecules. The generated Raman signal was focused onto the entrance slit of an imaging spectrometer (Shamrock 500i, Andor) with the resolution of <2 cm^{-1} for spectral analysis. To obtain a high SNR, various filters (e.g., dichroic mirror, bandpass filter, interference filter, edgepass filter, and notch filter) were selectively used in our experiment, and the angles of filters were optimized carefully. While recording Raman spectra, the integration time was set as 60 seconds.

It is worth stressing that two specific designs are adopt in our experiment to enhance detection sensitivity and stability. On the one hand, the time delay τ between the pump and seed pulses was taken as hundreds of femtoseconds, which is longer than durations of the pump and seed pulses but much shorter than the gain lifetime of N_2^+ lasing as well as the dephasing time of Raman coherence. If the time delay is too long, air lasing intensity and Raman coherence will significantly decrease, eventually resulting in degradation of Raman signals. If the time delay is too short, cross phase modulation between pump and seed pulses will produce the strong background noise. Thus, an optimal delay enables

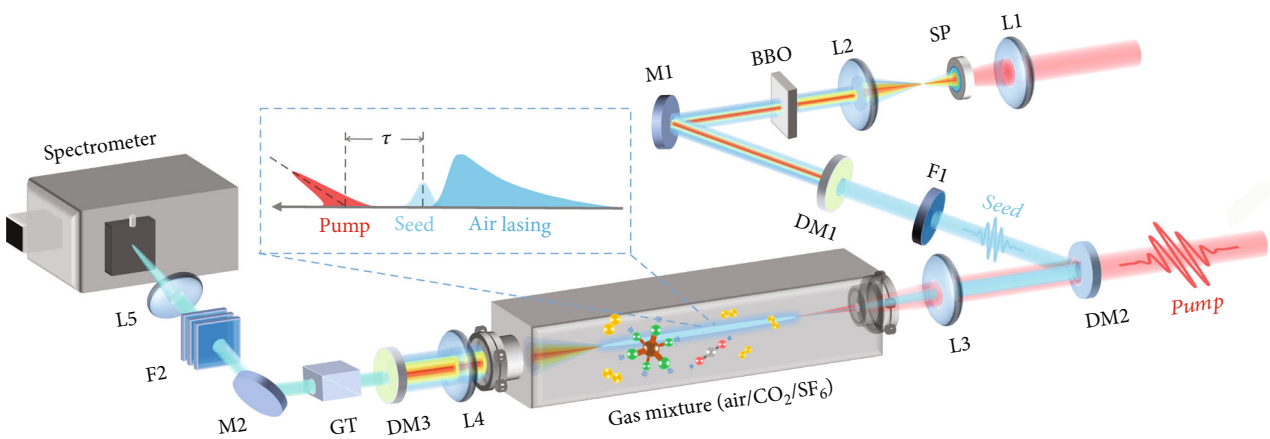

FIGURE 1: Experimental setup. M1, M2: reflective mirror; L1-L5: lens; SP: sapphire plate; BBO: beta barium borate; DM1-DM3: dichroic mirror; GT: Glan-Taylor prism; F1: narrowband filter with the central wavelength of 428 nm and the bandwidth of 1 nm; F2: combination of variable filters for recording the Raman signal at different wavelengths. Schematic diagram of the polarization states and time sequences of pump, seed and air lasing is shown in inset.

us to suppress the nonresonant background without the sacrifice of the CARS strength. On the other hand, the polarizations of pump and seed pulses were set as perpendicular to each other. Since the polarization of CARS signal always follows that of the seed pulse, such a polarization configuration enables us to eliminate the supercontinuum background by placing a Glan-Taylor prism before the spectrometer. The efficient suppression of supercontinuum radiation brought by filamentation greatly improves the SNR and stability. For clarity, the inset of Figure 1 shows the polarization states and time sequences of pump, seed, and air lasing. These unique designs endow our technique with high sensitivity.

2.2. Basic Principle. The basic principle of air-lasing-assisted CARS spectroscopy for high-sensitivity gas detection is shown in Figure 2. Typically, three laser beams (pump, Stokes, and probe) are required to produce CARS signals. In our scheme, the intense femtosecond pump laser can directly excite Raman coherence due to the pulse self-compression during filamentation [40]. As shown in Figure 2(b), the spectral width of the pump laser after nonlinear propagation has reached 3800 cm^{-1}, which is more than one order of magnitude width of the original spectrum. Such a broad spectrum allows for impulsive excitation of vibrational coherence of CO_2 and SF_6 molecules. Another pivotal role of the pump laser is to induce the optical gain of N_2^+, giving rise to the giant amplification of a delayed seed pulse. As presented in Figure 2(c), the external seed is amplified by three orders of magnitude at the wavelength of 427.8 nm, which corresponds to the characteristic transition from $B^2\Sigma_u^+(v'=0)$ to $X^2\Sigma_g^+(v=1)$ states. The low population on $X^2\Sigma_g^+(v=1)$ state facilitates the build-up of population inversion, leading to strong N_2^+ lasing generation in air [27]. The seed-amplified N_2^+ lasing exhibits a spectral bandwidth of ~13 cm^{-1}, a divergence full angle of ~45 mrad and a donut-shaped spatial profile. Moreover, as illustrated in the inset of Figure 1, N_2^+ lasing shows a temporal structure with a sharp rising edge and a slow falling edge as well as an inherent delay with the respect to the pump and seed pulses [31, 32]. All these superior properties make N_2^+ air lasing suitable for probing coherent vibrations of target molecules. The joint contributions of femtosecond laser filamentation and the filament-induced air lasing led to generation of strong CARS signals. The corresponding energy-level diagram was illustrated in Figure 2(a).

3. Results and Discussion

Figure 3 shows typical CARS spectra recorded in the mixture of standard air and CO_2 or SF_6, where the spectrum obtained in the standard air has been subtracted as background. The pump-seed delay was chosen at ~800 fs. The zero delay is defined as the moment at which N_2^+ lasing is the strongest. When the standard air was mixed with CO_2 gas with the 0.5% volume concentration, we can clearly observe two peaks with the frequency shifts of 1388 cm^{-1} and 1286 cm^{-1} (see Figure 3(a)), which correspond to Raman signals from CO_2 [41]. It is noteworthy that the peak around 993 cm^{-1} originates from insufficient background subtraction. When the standard air was mixed with 0.1% SF_6, a Raman peak with the frequency shift of 773 cm^{-1} was clearly observed, as shown in Figure 3(b). The measured Raman shift matches well with the characteristic frequency of nondegenerate stretching mode with A_{1g} symmetry of SF_6 [42]. It is noteworthy that these Raman peaks inherit the spectral feature of N_2^+ lasing, enabling the high spectral resolution in the gas detection. We performed the same measurement in the mixture of standard air, 0.5% CO_2, and 0.1% SF_6. As shown in Figure 3(c), Raman peaks of CO_2 and SF_6 molecules can be clearly distinguished. Moreover, the Raman signal intensity obtained in the gas mixture with two greenhouse gases is almost the same as that in the mixture with one greenhouse gas. It indicates that Raman signals from CO_2 and SF_6 do not affect each other, our method thus enables simultaneous measurement of multiple species.

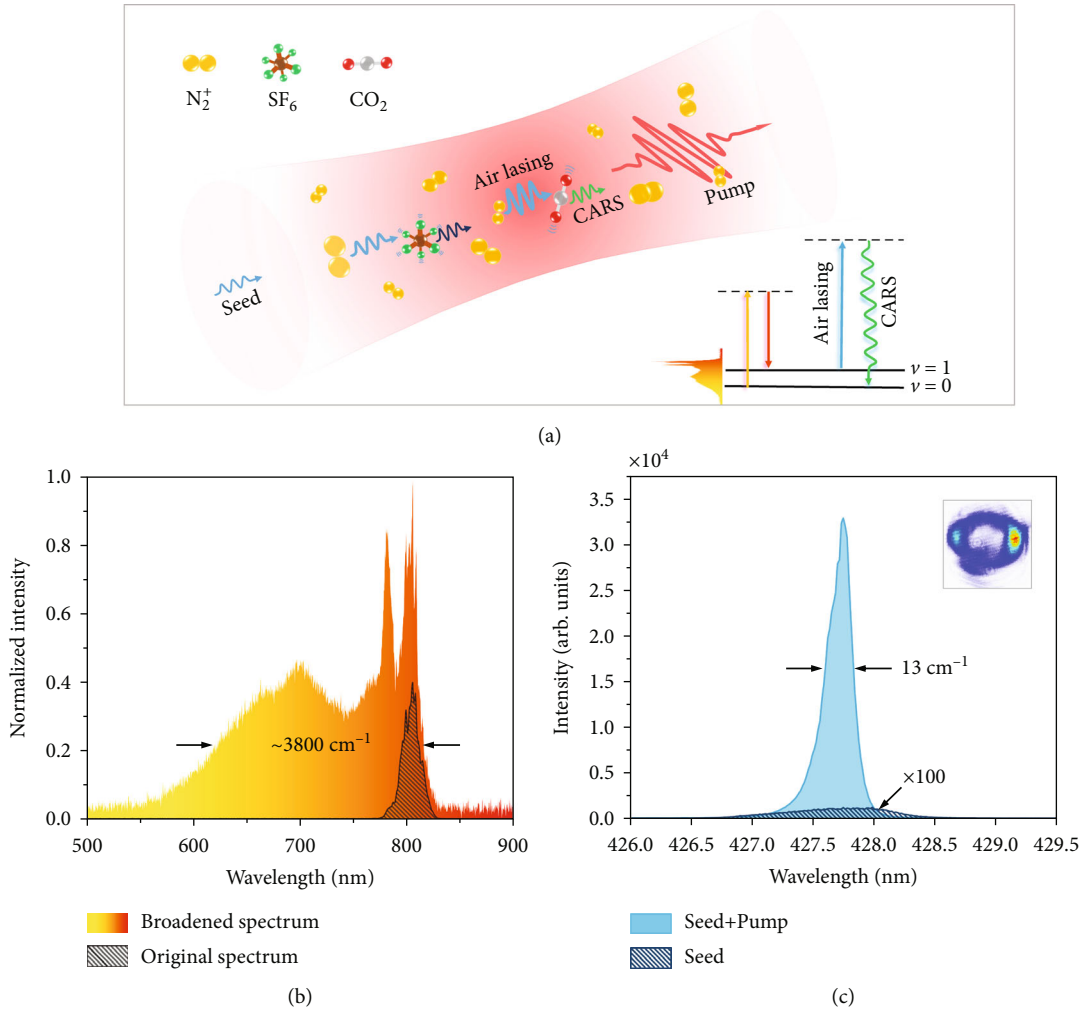

Figure 2: Basic principle for the greenhouse gas detection with air-lasing-based Raman spectroscopy. (a) The generation scheme of N_2^+ lasing and coherent anti-Stokes Raman scattering induced by the femtosecond pump pulse and the delayed seed pulse. (b) The original and broadened spectra of the pump laser. (c) The spectrum and spatial profile of seed-amplified N_2^+ lasing. For comparison, the initial spectrum of seed is indicated by the gray shaded region.

We further measured the quantitative relation between the Raman signal intensity of CO_2 and SF_6 and the corresponding gas pressures. It should be emphasized that the intensity of N_2^+ lasing almost remains unchanged within the measured pressure range, making the quantitative measurement credible. Figure 4(a) shows that CARS signals from CO_2 with the frequency shift of 1286 cm^{-1} and 1388 cm^{-1} exhibit a quadratic growth with the increase of CO_2 gas pressure, which is in good agreement with the theoretical predication and previous observation [43]. For Raman peaks at 1286 cm^{-1} and 1388 cm^{-1}, the lowest CO_2 pressure used in our experiment is 250 Pa and 100 Pa, respectively. The corresponding volume concentration is estimated as 0.25% and 0.1%. At such low concentrations, the SNR is still sufficient to distinguish CARS signal from the background noise, as shown in inset of Figure 4(a). We performed similar measurements in the mixture of standard air and SF_6. Likewise, the CARS signal from SF_6 gas also shows a quadratic dependence on gas pressure, as shown in Figure 4(b). In comparison with CO_2, SF_6 has a larger Raman cross section [44], and its vibrational period is closer to the pulse duration of the 800 nm laser. These factors make SF_6 molecules have a higher Raman excitation efficiency than CO_2 molecules, enabling us to observe CARS signal in the lower SF_6 gas concentration. The inset of Figure 4(b) shows the spectrum recorded in the gas mixture with standard air and 30 Pa SF_6. For SF_6 molecules, the detection limit has reached 0.03%.

In addition, the signal stability is crucial to high-sensitivity gas detection in the atmospheric environment. A key factor to affect the Raman signal stability is the stability of background spectrum recorded in standard air. In our scheme, supercontinuum radiation of the pump laser, as the main background noise, has been effectively suppressed by adopting perpendicular polarization configuration. As a result, background spectra exhibit small fluctuation, allowing for the background subtraction with the averaged value of multiple measurements. To quantitatively show the

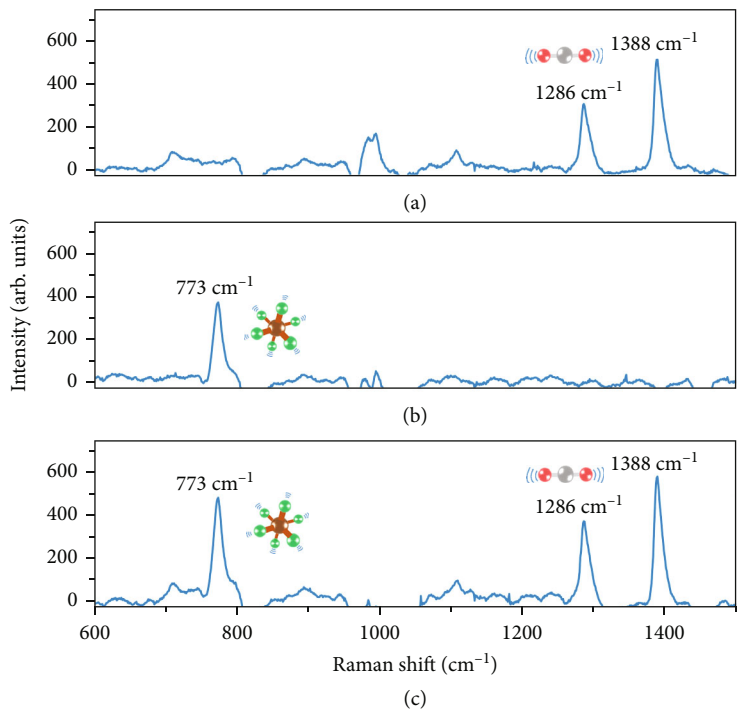

Figure 3: Typical Raman spectra. CARS spectra measured in the mixture of standard air and (a) 0.5% CO_2, (b) 0.1% SF_6, (c) 0.5% CO_2 and 0.1% SF_6, respectively. All spectra have subtracted the background spectrum taken in standard air.

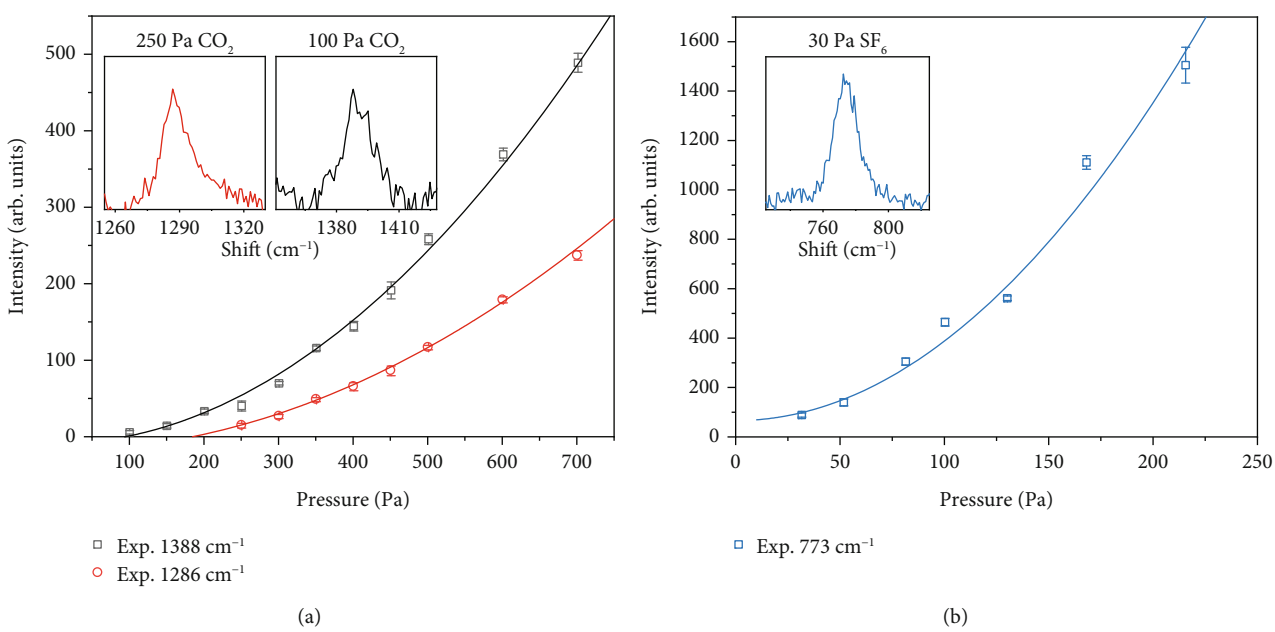

Figure 4: The intensity of Raman signal as a function of gas pressure. The dependence of CARS signals of (a) CO_2 and (b) SF_6 on the gas pressure. All CARS signals measured at different pressures can be well fitted by quadratic functions, as indicated by solid lines. Inset in (a) shows CARS signals with the frequency shift of 1388 cm^{-1} and 1286 cm^{-1} recorded in the gas mixture containing the 100-Pa and 250-Pa CO_2, respectively. Inset in (b) shows CARS signal recorded in the gas mixture containing the 30-Pa SF_6. Figures 4(a) and 4(b) were obtained at the pump-seed delay of 800 fs and 333 fs, respectively.

stability of Raman signal, we performed multiple measurements for Raman spectra at different gas pressures and indicated their standard deviations by error bars in Figure 4. The signal fluctuation can be quantitatively calculated using the ratio of the standard deviation and the average signal intensity. It is found that the signal fluctuation is closely related to gas pressure, more specifically, signal-to-noise ratio. In the measured pressure range, the minimum fluctuation of Raman signal is estimated to be about 2% for both SF_6 and CO_2 molecules.

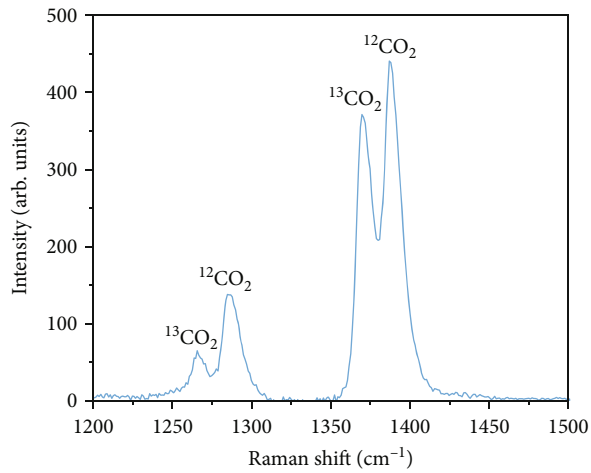

FIGURE 5: Raman signals from $^{12}CO_2$ and $^{13}CO_2$. The CARS spectrum was captured in the mixture of standard air, ~0.4% $^{12}CO_2$, and ~0.4% $^{13}CO_2$, in which the spectrum obtained with the 800 nm laser alone has been subtracted as background.

At last, we will show that the air-lasing-assisted CARS technique can be used for isotopic identification due to its high spectral resolution. It is well known that the carbon isotope plays an important role in geology science [45], environmental monitoring [46], and biological standardization [47]. We thus choose the carbon isotopologues of CO_2 (i.e., $^{12}CO_2$ and $^{13}CO_2$) as an example. Figure 5 shows the CARS spectrum obtained in the mixture of standard air, ~0.4% $^{12}CO_2$, and ~0.4% $^{13}CO_2$. Besides two characteristic Raman peaks of $^{12}CO_2$ at 1388 cm^{-1} and 1286 cm^{-1} as observed in Figure 3(a), we also clearly observed additional two peaks with the frequency shift of 1370 cm^{-1} and 1266 cm^{-1}, which are assigned to Raman signals of $^{13}CO_2$ [41]. Apparently, we can well distinguish the isotopologues of CO_2 with the air-lasing-assisted CARS technique, which benefits from the narrow spectrum of air lasing.

From the measured spectra in Figure 5, the branching ratios of $^{12}CO_{12}$ and $^{13}CO_2$ Raman peaks are estimated to be 2.1 and 1.2 for weak Raman peaks below 1300 cm^{-1} and strong Raman peaks above 1300 cm^{-1}, respectively. The striking difference in branching ratio mainly originates from different intensity ratios of the ν_1, $2\nu_2$ Fermi diads of $^{12}CO_2$ and $^{13}CO_2$ [48]. In addition, we can clearly see that the Raman signals of $^{13}CO_2$ are always weaker than that of $^{12}CO_2$, regardless of strong and weak Raman peaks. It could be attributed to different Raman scattering cross-sections of $^{12}CO_2$ and $^{13}CO_2$ [41], which is closely related to energy-level structures of molecules. Quantitative measurements on the concentration ratio of $^{12}CO_2$ and $^{13}CO_2$ will be performed in the future work. It is noteworthy that the analysis of the carbon isotope has been performed with Raman spectroscopy in the previous study [41], but the measurement was done in the high-pressure gas. In contrast, air-lasing-assisted CARS technique can identify the carbon isotope in the mixture of air and low-concentration CO_2. In principle, the approach can be applied to identification of other isotopes as long as the Raman frequency difference of isotopologues is larger than the spectral width of air lasing.

Experimental results above clearly show that air-lasing-assisted CARS technique can be used for quantitative measurements of greenhouse gas concentration. The signal-to-noise ratio of Raman scattering is enhanced significantly via the choice of orthogonal polarization and the optimization of pump-seed delay. Moreover, signal fluctuations brought by supercontinuum generation in previous method [39] are largely suppressed. However, in contrast to conventional methods of atmospheric sensing, e.g., differential absorption Lidar (DIAL), the sensitivity of the current method is at least 3 orders of magnitude lower [49]. Thus, the sensitivity of this method needs to be enhanced greatly for the realistic application in the trace gas detection. The further improvement in the sensitivity is expected by using a pump laser with a higher energy, higher repetition, higher stability, and shorter pulse duration. Particularly, the shorter laser pulse will greatly enhance Raman excitation efficiency because the broad spectral coverage makes more photons participate in the creation of vibrational coherence. It is noteworthy that although the DIAL technique has a very high sensitivity, it can only measure a single specific species by choosing a couple of laser wavelengths around the molecular absorption. Our method is able to simultaneously detect a large number of molecules, allowing for gas sensing without the need for an a priori knowledge of molecules to detect. This is a major advantage of our method in contrast to conventional methods.

In addition, for the standoff detection, the two-beam design is expected to simplify as a single beam. Very recently, we use N_2 lasing instead of N_2^+ lasing to develop single-beam coherent Raman spectroscopy [50]. Owing to strong quenching effect of oxygen gas for N_2 lasing, the sensitivity of N_2-lasing-assisted coherent Raman spectroscopy is one order of magnitude lower than the current scheme. Thus, it is our next goal to develop single-beam coherent Raman spectroscopy with the sensitivity on the level of 10^{-6}, which will provide a powerful tool for chemical identification, gas detection, and combustion diagnosis.

4. Conclusion

In conclusion, we have demonstrated a novel coherent Raman spectroscopy for high-sensitive gas detection taking advantage of filament-induced air lasing. The nonlinear spectroscopy inherits all advantages of the hybrid fs/ps CARS technique. Moreover, the utilization of air lasing avoids complex spectral tailoring. It is demonstrated that such a simplified fs/ps CARS technique has the ability of the high-sensitivity detection, simultaneous measurement of multiple pollutants, and the identification of carbon isotope. The detection limits of CO_2 and SF_6 greenhouse gas concentrations have reached 0.1% and 0.03%, respectively. The air-lasing-assisted Raman spectroscopy offers a versatile method for high-sensitivity detection of gas pollutants and greenhouse gas but also opens the possibility towards the rapid detection of epidemics such as COVID-19 at a safe distance [51].

Data Availability

The data that support the findings of this study are available from the corresponding authors upon reasonable request.

Conflicts of Interest

The authors declare that there is no conflict of interest regarding the publication of this article.

Authors' Contributions

J. Yao conceived the idea and designed the experiment. Y. Cheng and Z. Xu supervised the project. Z. Zhang, F. Zhang, and B. Xu performed the experiment. Z. Zhang, F. Zhang, X. Lu, and J. Yao analyzed the results. All authors contributed to the preparation of the manuscript and reviewed the manuscript. Zhihao Zhang and Fangbo Zhang contributed equally to this work.

Acknowledgments

This work is supported by the National Natural Science Foundation of China (11822410, 12034013, 12074063); Key Research Program of Frontier Sciences of Chinese Academy of Sciences (QYZDJ-SSW-SLH010); Program of Shanghai Academic Research Leader (20XD1424200); Shanghai Municipal Science and Technology Major Project (2019SHZDZX01); and Youth Innovation Promotion Association of CAS (2018284).

References

[1] A. Braun, G. Korn, X. Liu, D. Du, J. Squier, and G. Mourou, "Self-channeling of high-peak-power femtosecond laser pulses in air," *Optics Letters*, vol. 20, no. 1, pp. 73–75, 1995.

[2] A. Couairon and A. Mysyrowicz, "Femtosecond filamentation in transparent media," *Physics Reports*, vol. 441, no. 2-4, pp. 47–189, 2007.

[3] S. L. Chin, T. Wang, C. Marceau et al., "Advances in intense femtosecond laser filamentation in air," *Laser Physics*, vol. 22, no. 1, pp. 1–53, 2012.

[4] H. Xu, Y. Cheng, S. L. Chin, and H. Sun, "Femtosecond laser ionization and fragmentation of molecules for environmental sensing," *Laser & Photonics Reviews*, vol. 9, no. 3, pp. 275–293, 2015.

[5] J. P. Wolf, "Short-pulse lasers for weather control," *Reports on Progress in Physics*, vol. 81, no. 2, article 026001, 2018.

[6] Y. Su, W. Zhang, S. Chen et al., "Engineering black titanium dioxide by femtosecond laser filament," *Applied Surface Science*, vol. 520, p. 146298, 2020.

[7] H. Zang, H. Li, W. Zhang et al., "Robust and ultralow-energy-threshold ignition of a lean mixture by an ultrashort-pulsed laser in the filamentation regime," *Light: Science & Applications*, vol. 10, no. 1, p. 49, 2021.

[8] G. Méjean, J. Kasparian, J. Yu, S. Frey, E. Salmon, and J. P. Wolf, "Remote detection and identification of biological aerosols using a femtosecond terawatt lidar system," *Applied Physics B: Lasers and Optics*, vol. 78, no. 5, pp. 535–537, 2004.

[9] H. Xu, J. Daigle, Q. Luo, and S. L. Chin, "Femtosecond laser-induced nonlinear spectroscopy for remote sensing of methane," *Applied Physics B: Lasers and Optics*, vol. 82, no. 4, pp. 655–658, 2006.

[10] H. Xu, Y. Kamali, C. Marceau et al., "Simultaneous detection and identification of multigas pollutants using filament-induced nonlinear spectroscopy," *Applied Physics Letters*, vol. 90, no. 10, p. 101106, 2007.

[11] H. Xu and S. L. Chin, "Femtosecond laser filamentation for atmospheric sensing," *Sensors*, vol. 11, no. 1, pp. 32–53, 2011.

[12] J. Kasparian, M. Rodríguez, G. Méjean et al., "White-light filaments for atmospheric analysis," *Science*, vol. 301, no. 5629, pp. 61–64, 2003.

[13] F. El-Diasty, "Coherent anti-Stokes Raman scattering: spectroscopy and microscopy," *Vibrational Spectroscopy*, vol. 55, no. 1, pp. 1–37, 2011.

[14] J. H. Odhner, E. T. McCole, and R. J. Levis, "Filament-driven impulsive Raman spectroscopy," *The Journal of Physical Chemistry. A*, vol. 115, no. 46, pp. 13407–13412, 2011.

[15] B. D. Prince, A. Chakraborty, B. M. Prince, and H. U. Stauffer, "Development of simultaneous frequency- and time-resolved coherent anti-Stokes Raman scattering for ultrafast detection of molecular Raman spectra," *The Journal of Chemical Physics*, vol. 125, no. 4, article 044502, 2006.

[16] J. D. Miller, M. N. Slipchenko, T. R. Meyer, H. U. Stauffer, and J. R. Gord, "Hybrid femtosecond/picosecond coherent anti-Stokes Raman scattering for high-speed gas-phase thermometry," *Optics Letters*, vol. 35, no. 14, pp. 2430–2432, 2010.

[17] S. P. Kearney, "Hybrid fs/ps rotational CARS temperature and oxygen measurements in the product gases of canonical flat flames," *Combustion and Flame*, vol. 162, no. 5, pp. 1748–1758, 2015.

[18] B. D. Patterson, Y. Gao, T. Seeger, and C. J. Kliewer, "Split-probe hybrid femtosecond/picosecond rotational CARS for time-domain measurement of S-branch Raman linewidths within a single laser shot," *Optics Letters*, vol. 38, no. 22, pp. 4566–4569, 2013.

[19] A. Dogariu, J. B. Michael, M. O. Scully, and R. B. Miles, "High-gain backward lasing in air," *Science*, vol. 331, no. 6016, pp. 442–445, 2011.

[20] J. Yao, B. Zeng, H. Xu et al., "High-brightness switchable multiwavelength remote laser in air," *Physical Review A*, vol. 84, no. 5, article 051802, 2011.

[21] J. Yao, G. Li, C. Jing et al., "Remote creation of coherent emissions in air with two-color ultrafast laser pulses," *New Journal of Physics*, vol. 15, no. 2, article 023046, 2013.

[22] D. Kartashov, S. Alisauskas, A. Baltuska, A. Schmitt-Sody, W. Roach, and P. Polynkin, "Remotely pumped stimulated emission at 337 nm in atmospheric nitrogen," *Physical Review A*, vol. 88, no. 4, article 041805, 2013.

[23] S. Mitryukovskiy, Y. Liu, P. Ding, A. Houard, and A. Mysyrowicz, "Backward stimulated radiation from filaments in nitrogen gas and air pumped by circularly polarized 800 nm femtosecond laser pulses," *Optics Express*, vol. 22, no. 11, pp. 12750–12759, 2014.

[24] H. Xu, E. Lötstedt, A. Iwasaki, and K. Yamanouchi, "Sub-10-fs population inversion in N_2^+ in air lasing through multiple state coupling," *Nature Communications*, vol. 6, article 8347, 2015.

[25] J. Yao, S. Jiang, W. Chu et al., "Population redistribution among multiple electronic states of molecular nitrogen ions in strong laser fields," *Physical Review Letters*, vol. 116, no. 14, p. 143007, 2016.

[26] P. Polynkin and Y. Cheng, "Air Lasing," in *Springer Series in Optical Sciences*, vol. 208, Springer International Publishing, 2018.

[27] J. Yao, W. Chu, Z. Liu, J. Chen, B. Xu, and Y. Cheng, "An anatomy of strong-field ionization-induced air lasing," *Applied Physics B: Lasers and Optics*, vol. 124, no. 5, p. 73, 2018.

[28] L. Yuan, Y. Liu, J. Yao, and Y. Cheng, "Recent advances in air lasing: a perspective from quantum coherence," *Advanced Quantum Technologies*, vol. 2, no. 11, p. 1900080, 2019.

[29] H. Li, M. Hou, H. Zang et al., "Significant enhancement of N_2^+ lasing by polarization-modulated ultrashort laser pulses," *Physical Review Letters*, vol. 122, no. 1, article 013202, 2019.

[30] Q. Zhang, H. Xie, G. Li et al., "Sub-cycle coherent control of ionic dynamics via transient ionization injection," *Communications Physics*, vol. 3, no. 1, p. 50, 2020.

[31] G. Li, C. Jing, B. Zeng et al., "Signature of superradiance from a nitrogen-gas plasma channel produced by strong-field ionization," *Physical Review A*, vol. 89, no. 3, article 033833, 2014.

[32] Y. Liu, P. Ding, G. Lambert, A. Houard, V. Tikhonchuk, and A. Mysyrowicz, "Recollision-induced superradiance of ionized nitrogen molecules," *Physical Review Letters*, vol. 115, no. 13, p. 133203, 2015.

[33] P. Ding, E. Oliva, A. Houard, A. Mysyrowicz, and Y. Liu, "Lasing dynamics of neutral nitrogen molecules in femtosecond filaments," *Physical Review A*, vol. 94, no. 4, article 043824, 2016.

[34] J. Ni, W. Chu, H. Zhang et al., "Impulsive rotational Raman scattering of N_2 by a remote "air laser" in femtosecond laser filament," *Optics Letters*, vol. 39, no. 8, pp. 2250–2253, 2014.

[35] P. N. Malevich, R. Maurer, D. Kartashov et al., "Stimulated Raman gas sensing by backward UV lasing from a femtosecond filament," *Optics Letters*, vol. 40, no. 11, pp. 2469–2472, 2015.

[36] B. Xu, J. Yao, Y. Wan et al., "Vibrational Raman scattering from coherently excited molecular ions in a strong laser field," *Optics Express*, vol. 27, no. 13, pp. 18262–18272, 2019.

[37] Z. Liu, J. Yao, H. Zhang et al., "Extremely nonlinear Raman interaction of an ultrashort nitrogen ion laser with an impulsively excited molecular wave packet," *Physical Review A*, vol. 101, no. 4, article 043404, 2020.

[38] G. Li, H. Xie, Q. Zhang et al., "Enhanced resonant vibrational Raman scattering of N_2^+ induced by self-seeding ionic lasers created in polarization-modulated intense laser fields," *Optics Letters*, vol. 45, no. 19, pp. 5616–5619, 2020.

[39] X. Zhao, S. Nolte, and R. Ackermann, "Lasing of N_2^+ induced by filamentation in air as a probe for femtosecond coherent anti-Stokes Raman scattering," *Optics Letters*, vol. 45, no. 13, pp. 3661–3664, 2020.

[40] J. Odhner, D. A. Romanov, and R. J. Levis, "Rovibrational wave-packet dispersion during femtosecond laser filamentation in air," *Physical Review Letters*, vol. 103, no. 7, article 075005, 2009.

[41] J. Li, R. Li, B. Zhao et al., "Quantitative measurement of carbon isotopic composition in CO_2 gas reservoir by Micro-Laser Raman spectroscopy," *Spectrochimica Acta Part A*, vol. 195, pp. 191–198, 2018.

[42] S. Akhmanov, S. Gladkov, M. Karimov, N. Koroteev, V. Zadkov, and G. Marowsky, "CARS thermometry of polyatomic gases: SF_6," *IEEE Journal of Quantum Electronics*, vol. 20, no. 4, pp. 424–428, 1984.

[43] A. Dogariu, A. Goltsov, H. Xia, and M. O. Scully, "Concentration dependence in coherent Raman scattering," *Journal of Modern Optics*, vol. 55, no. 19-20, pp. 3255–3261, 2008.

[44] H. Inaba and T. Kobayasi, "Laser-Raman radar — Laser-Raman scattering methods for remote detection and analysis of atmospheric pollution," *Opto-Electronics*, vol. 4, no. 2, pp. 101–123, 1972.

[45] F. M. Gradstein, J. G. Ogg, M. D. Schmitz, and G. M. Ogg, *The Geologic Time Scale 2012*, Elsevier, 2012.

[46] J. P. Ferrio, J. Voltas, and J. L. Araus, "Use of carbon isotope composition in monitoring environmental changes," *Management of Environmental Quality*, vol. 14, no. 1, pp. 82–98, 2003.

[47] C. Wang and P. Sahay, "Breath analysis using laser spectroscopic techniques: breath biomarkers, spectral fingerprints, and detection limits," *Sensors*, vol. 9, no. 10, pp. 8230–8262, 2009.

[48] H. E. Howard-Lock and B. P. Stoicheff, "Raman intensity measurements of the Fermi diad ν_1, $2\nu_2$ in $^{12}CO_2$ and $^{13}CO_2$," *Journal of Molecular Spectroscopy*, vol. 37, no. 2, pp. 321–326, 1971.

[49] D. A. Vallero, *Environmental Systems Science: Theory and Practical Applications*, Elsevier, 2021.

[50] F. Zhang, H. Xie, L. Yuan et al., "Background-free single-beam coherent Raman spectroscopy assisted by air lasing," *Optics Letters*, vol. 47, no. 3, pp. 481–484, 2022.

[51] C. Carlomagno, D. Bertazioli, A. Gualerzi et al., "COVID-19 salivary Raman fingerprint: innovative approach for the detection of current and past SARS-CoV-2 infections," *Scientific Reports*, vol. 11, no. 1, p. 4943, 2021.